Elemental abundances in CEMP stars: r- and s- process elements

Aruna Goswami, Subramania Athiray P, Drisya K

Indian Institute of Astrophysics, Bangalore 560034; aruna@iiap.res.in

Summary. A number of Carbon-Enhanced Metal-poor (CEMP) stars are known to exhibit enhancement of both $r-$ and $s-$process elements. An understanding of their relative contributions would provide insight into the production mechanisms and nucleosynthetic sites and origins of the heavy elements observed in the stars. We have investigated ways to delineate the observed abundances into their respective r- and s-process contributions. Preliminary results obtained using appropriate model functions in the framework of a parametric model are discussed.

Keywords: stars: giants, AGB, nucleosynthesis, abundances

1 Introduction

CEMP stars are classified as CEMP-s or CEMP-r based on the observed enhancement of abundances of heavy elements of s- and r- process respectively. These elements are formed primarily by captures of neutrons by iron-peak seeds; however, recent studies by several authors[1,2,3] have predicted efficient production of the third peak s-process element lead (Pb) in very metal-poor environments characterized by lack of iron-seed nuclei.

Production mechanisms of s- and r-process require not only two widely different astrophysical sites but also very different time scales. They also require different neutron fluxes; the time scale for neutron capture by iron-seed elements for s-process is much longer than that required for their beta decay and in r-process much shorter than the beta decay time scale. Identification of an explicit stellar site for $s-$process nucleosynthesis started with the works of Weigert[4] and Schwarzchild and Harm[5] on the thermal pulse calculations. Slow neutron-capture elements are now believed to be produced due to partial mixing of protons into the radiative C-rich layers during thermal pulses that initiate the chain of reactions $^{12}C(p,\gamma)^{13}N(\beta)$ $^{13}C(\alpha ,n)^{16}O$ in a narrow mass region of the He intershell during the inter-pulse phases of a low-mass AGB star. Rapid neutron-capture process elements are thought to be produced during SN explosions or neutron star mergers.

Classification and analysis of a number of CEMP stars in the recent past provided evidence of enhancement of both $s-$ and $r-$elements[6,7,8,9,10] The upper limit in the metallicity of stars showing double enhancement is [Fe/H] ≤ -2 (HE 1305+0007 with [Fe/H] =-2.0, Goswami[8] et al.). In spite of several efforts, a physical explanation for the observed double enhancement is still lacking [11,12].

Heavy element abundances in the solar system have contributions from both $r-$ and $s-$process in different proportions. The first step to understand the nucleosynthetic origin of the heavy elements is to determine the relative contributions from the $s-$ and $r-$process to the observed abundances. We have investigated ways to delineate the observed abundances into their respective $r-$ and $s-$ process contributions. Identification of the dominent processes contributing to the heavy element abundances in CEMP stars is likely to provide clues to the physical mechanism(s) responsible for the observed double enhancements in these objects.

2 A parametric model based analysis

There have been several efforts to explain the solar system abundances of elements associated with slow neutron capture process. One of the early models that could reproduce the observed solar system σN curve with a good agreement is the parametric model of Howard[13] et al. The model used an exponential distribution of neutron exposures via sequential irradiations. A fit for solar system σN curve was obtained by optimizing the neutron density and temperature which in turn optimized the mean neutron exposure. This model was used by Aoki[14] et al. to study s-process elemental abundances in metal-poor stars. Bo Zhang[15] et al. also utilized parametric model to explain the observed abundances of metal-poor double enhanced stars. We have explored the origin of neutron-capture elements by comparing the observed abundances with the predicted $s-$ and $r-$ process contribution using appropriate model function in the framework of a parametric model.

2.1 Methodology

We have utilized the solar system $r-$ and $s-$ process isotopic abundances of Arlandini[16] et al.'s stellar model. The observed elemental abundances are scaled to the metallicity of the corresponding CEMP stars and normalized to their respective barium abundances. Elemental abundances are then fitted with the parametric model functions

$$log\epsilon_i = A_s N_{s,i} + A_r N_{r,i} \quad (1)$$

$$log\epsilon_i = A_s N_{s,i} + (1 - A_s) N_{r,i} \quad (2)$$

for the stars listed in Table 1. A_s and A_r are the component coefficients that correspond to contributions from the $s-$ and $r-$process respectively. $N_{s,i}$ and $N_{r,i}$ are the i^{th} element abundance produced by $s-$ and $r-$process respectively. The best fit curve obtained for HE 1305+0007 and HD 5223 are shown in Fig 3 and 4 respectively. The observed abundances for HE 1305+0007 and HD 5223 are taken from Goswami[8] et al; for all other stars listed in Table 1, the observed abundances are taken from Jonsell[10] et al's. compilation (Table 8).

Table 1. Best fit co-efficients and reduced χ^2 values for a sample of CEMP stars

Star name	Best fit values for $\log\epsilon = A_s N_s + A_r N_r$			Best fit values for $\log\epsilon = A_s N_s + (1 - A_s) N_r$	
	A_s	A_r	χ^2	A_s	χ^2
HE1305+0007(r+s)	0.47±0.11	0.53±0.09	1.07	0.75±0.08	0.94
HD5223(CH)	0.60±0.20	0.37±0.16	1.12	0.66±0.15	1.46
HD209621(r+s)	0.57±0.10	0.42±0.08	1.08	0.47±0.08	1.94
LP625-44(r+s)	0.78±0.01	0.05±0.07	1.43	1.01±0.06	2.11
CS31062-012(r +s)	0.60±0.08	0.39±0.08	1.11	0.60±0.07	0.84
CS22898-027(r +s)	0.56±0.07	0.41±0.05	1.19	0.60±0.05	1.14
HE2148-1247(r +s)	0.56±0.05	0.43±0.04	1.08	0.57±0.04	0.97
HE0338-3945(r +s)	0.60±0.05	0.38±0.05	0.96	0.63±0.05	0.94
CS22880-074(r +s)	0.73±0.08	0.22±0.07	1.29	0.76±0.07	1.74
HD196944(s)	0.861±0.08	0.08±0.12	1.30	1.01±0.06	0.29

2.2 Error analysis

Errors in the derived abundances arise mainly from two sources, random errors as well as systematic errors arising from uncertainties in the adopted atmospheric parameters. Both errors play important roles in deciding the goodness of fit of the parametric model function and hence the model. In most cases for the stars listed in Table 1, the metallicities are determined using Fe I and Fe II lines with an error in the range of ±0.2 to 0.3dex as indicated by the derived standard deviation σ. The abundances of the heavy elements are derived usually by spectrum synthesis calculations. Estimated fitting errors range between 0.1 and 0.3 dex. For the parametric model function fits we have adopted ±0.2 dex as the error in the observed abundance data for the stars HE 1305+0007, HD 5223, HD 209621 as given by Goswami[8] et al. (2006). For all other stras the errors are taken from the respective references given in Jonsell[10] et al.; for the star HD 196944 out of five references mentioned in

Jonsell et al.'s paper, the value given by Aoki et al. is adopted. The reported abundance of lead (Pb) in HD 5223 is quoted as an upper limit in Goswami[8] et al.; we have therefore used the lead abundance in this star as 1.95 instead of 2.15 given by the authors.

3 Results and Conclusions

The derived coefficients A_s andA_r from the model fits using parametric model function (1) are indicative of fractional contributions coming from the $s-$ and $r-$ process respectively.

HE 1305+0007 This star was first classified as a CEMP-r/s stars by Goswami[8] et al. Model calculation indicates that $r-$process contribution is slightly higher than that of the $s-$process with A_r = 0.53 ±0.09 and A_s = 0.47 ±0.11.

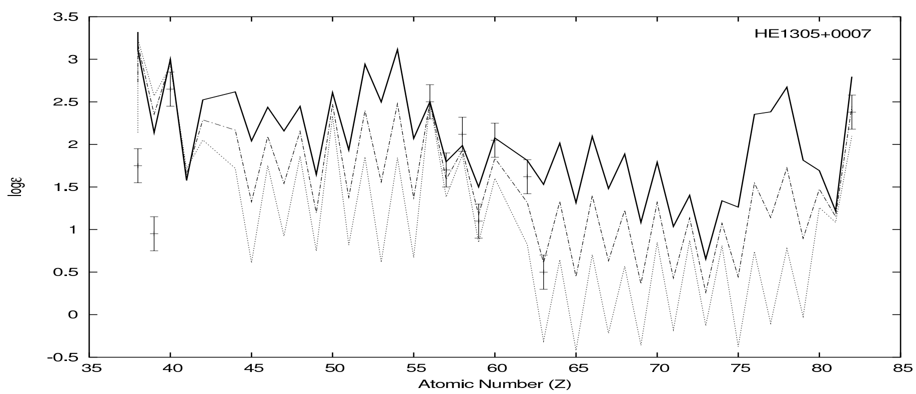

Fig. 1. Abundance patterns of heavy elements from Arlandini[15] (Stellar model). Solid line shows abundances due to only r-process; dotted line is of s-process only and dashed line indicates abundance pattern derived from a simple average of r- and s- processes. The patterns are normalized to Ba. The points with error bars are observed abundances in HE 1305+0007 and are taken from Goswami[8] et al.

HD 5223, HD 196944, LP 625-44, CS 22880-074 These stars belong to the CEMP-s group; they exhibit enhanced $s-$process elemental abundances. With a good agreement with observations, the dominancy of the $s-$ process

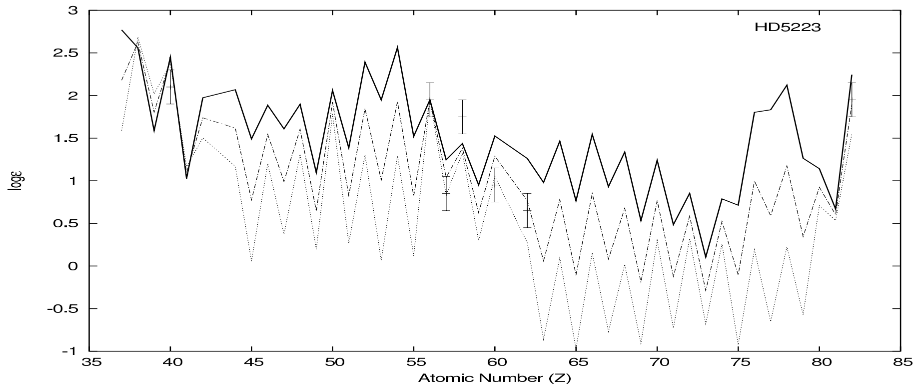

Fig. 2. Same as Fig 1, shown for HD 5223.

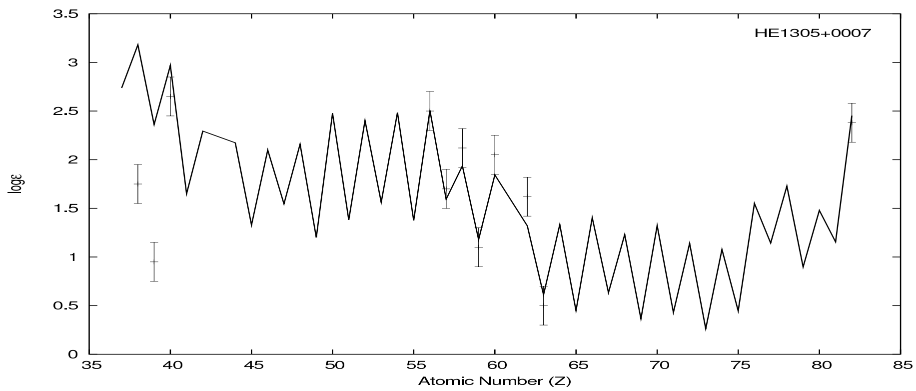

Fig. 3. The best fit curve obtained with the parametric model function $\log\epsilon_i = (A_s N_{s,i} + A_r N_{r,i})$. Observed abundances (points with error bars) in HE 1305+0007 are from Goswami[8] et al.

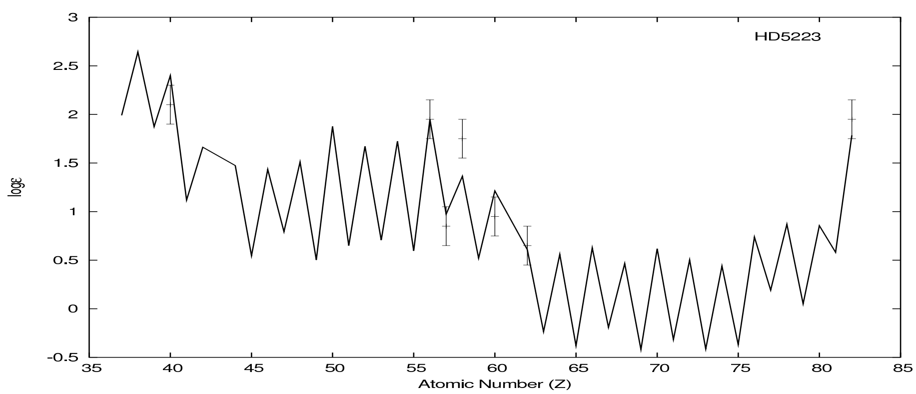

Fig. 4. Same as Fig 3, shown for HD 5223

in these objects is also noticed from the model analysis. The component coefficients of $s-$process are A_s = 0.60 ± 0.20, 0.86 ± 0.08, 0.78 ± 0.01 and 0.73 ± 0.08 respectively and the component coefficients of $r-$ process A_r are respectively 0.37 ± 0.16, 0.08 ± 0.12, 0.05 ± 0.07 and 0.22 ± 0.07.

HD 209621, CS 31062-012, CS 22898-027, HE 2148-1247, HE 0338-3945 In a recent high resolution spectroscopic analysis of the star HD 209621, the star is shown as CEMP-r/s star (Goswami et al. in preparation). The other four stars are listed as r+s stars in Jonsell[10] et al. (2006). Our model fits coefficients A_s for these objects are respectively 0.568 ± 0.10, 0.59 ± 0.08, 0.56 ± 0.07, 0.56 ± 0.05 and 0.60 ± 0.05; the corresponding A_r values are 0.42 ± 0.08, 0.39 ± 0.08, 0.40 ± 0.05, 0.43 ± 0.04 and 0.37 ± 0.05 respectively. As is noticed A_s values are slightly higher than the values of A_r in these stars except in HE 1305+0007 where the component coefficient A_r indicates dominancy of $r-$process over $s-$. Following CEMP stars classification scheme of Beers and Christlieb[17] these stars however fall into CEMP-r+s stars with [Ba/Eu] estimates as 0.35, 0.36, 0.35, 0.38 and 0.47 respectively. In this classification scheme C-enhanced stars with [Ba/Eu] $\geq$ 0.5 are classified as CEMP-s stars.

A precise knowledge of the dominant mode of production (either $s-$ or $r-$) of the heavy elements would help to identify and construct a consistent and a realistic physical scenario involving explicit production sites, enviroment and precise physical mechanism(s) that could explain the origin of this rare class of objects.

As evident from the resutls presented in Table 1, calculations carried out using model function (2) also show similar fractional contributions from $s-$ and $r-$ process in these objects. However, the constraint of making the sum of the coefficients A_s and A_r equal to unity strikes out the possibility of finding additional mechanisms which would have contributed to the observed abundances.

Funding from DST Project No. SR/S2/HEP-09/2007 is gratefully acknowledged.

References

1. R. Gallino, C Arlandini, M Busso et al. ApJ, **497**, 388 (1998)
2. S. Goriely, N. S. Mowlavi, A&A, **362**, 599 (2000)
3. M. Busso et al. ApJ, **557**, 802 (2001)
4. A. Weigert, ZA, **64**, 395 (1966)
5. M. Schwarzschild & R. Harm. ApJ, **150**, 961 (1967)
6. Aruna Goswami, MNRAS, **359**, 531 (2005)
7. V. Hill, B. Barbuy, M. Spite, F. Spite et al., A&A, **353**, 557 (2000)
8. Aruna Goswami, Wako Aoki, T C Beers et al., MNRAS, **372**, 343 (2006)
9. Aruna Goswami, P Bama, N S Shantikumar et al., BASI, **35**, 339 (2007)
10. Jonsell K, Barklem P. S. Gustafsson, B. et al.: **451**, 651, (2006)

11. Y. -Z. Qian, G. J. Wasserburg, ApJ, **588**, 1099 (2003)
12. S. Wanajo, k. Nomoto et. al. ApJ, **636**, 842 (2006)
13. W. A. Howard, G. J. Mathews, K. Takahashi et al., ApJ, **309**, 633 (1986)
14. Wako Aoki, Sean G. Ryan, John E. Norris et al., ApJ, **561**, 346 (2001)
15. Bo Zhang, Kun Ma, Guide Zhou, ApJ, **642**, 1075 (2006)
16. C. Arlandini, F. Kappeler, K Wisshak et al. ApJ, **525**, 886 (1999)
17. T. C. Beers & N. Christlieb, ARAA, **43**, 531 (2005)